ISSN 1063-780X, Plasma Physics Reports, 2006, Vol. 32, No. 3, pp. 254–261. © Pleiades Publishing, Inc., 2006.
Original Russian Text © N.V. Denisova, B.V. Postnikov, V.M. Fomin, 2006, published in Fizika Plazmy, 2006, Vol. 32, No. 3, pp. 281–288.

LOW-TEMPERATURE PLASMA

Transverse Glow Discharges in Supersonic Air and Methane Flows

N. V. Denisova, B. V. Postnikov, and V. M. Fomin

Institute of Theoretical and Applied Mechanics, Siberian Division, Russian Academy of Sciences, ul. Institutskaya 4/1, Novosibirsk, 630090 Russia

Received February 3, 2005; in final form, August 1, 2005

Abstract—Transverse glow discharges in supersonic air and methane flows are studied both experimentally and theoretically. The experiments show that a diffuse volume discharge filling the whole cross section of the flow can easily be initiated in air, whereas a diffuse discharge in a methane flow shows a tendency to transition into a constricted mode. The electron transport coefficients (mobility and drift velocity) and the kinetic coefficients (such as collisional excitation rates of the vibrational levels of a methane molecule, as well as dissociation and ionization rates) are calculated by numerically solving the Boltzmann equation for the electron energy distribution function. The calculated coefficients are used to estimate the parameters of the plasma and the electric field in the positive column of a discharge in methane.

PACS numbers: 52.80.–s, 52.80.Hc, 82.33.Xj

DOI: 10.1134/S1063780X06030081

1. INTRODUCTION

In recent years, discharges in supersonic and hypersonic gas flows at low pressures have attracted great interest. The possibility of using a low-temperature plasma to affect the boundary layer and the problem of controlling air flows around a body with the aim of decreasing the drag force have been actively studied. Such studies were performed, e.g., in [1–3], where the effect of a glow discharge on the parameters of a gas flow was investigated and the main parameters of the plasma of a longitudinal glow discharge in a supersonic air flow were determined. It was shown that a glow discharge initiated near a body placed in the gas flow substantially changes the flow pattern. The supersonic flow provided a rapid outflow of the gas from the discharge, thereby stabilizing it. The discharge characteristics were found to depend substantially on the power deposited in the discharge, the geometry and material of the electrodes, the flow velocity, etc.

A new direction of research is the development of novel methods for decomposing hydrocarbons in a nonequilibrium low-temperature plasma. The disadvantage of the existing pyrolytical methods, which make use of a thermodynamically equilibrium arc plasma, is high power consumption. The plasma temperature in plasmatrons reaches 3000–6000 K. Such a high temperature ensures the thermal dissociation of methane molecules and the formation of free radicals, which initiate subsequent chain chemical reactions. It is well known that, in a nonequilibrium plasma at moderate gas temperatures (400–700 K), free radicals are produced via a different mechanism—collisions of electrons with gas molecules. In this connection, the possibility of employing various sources of nonequilibrium plasma for natural gas processing has been extensively studied [4–7].

Among the pioneering studies, we can mention [4], where mechanisms for methane conversion in a glow discharge were investigated experimentally. The authors of [4] proposed a kinetic scheme for methane conversion that included the reaction of methane production in collisions of electrons with methane molecules. It was shown that ethane can be efficiently produced via decomposition of methane in a low-pressure glow discharge without deep cooling of the discharge tube. At present, much experimental and theoretical effort is devoted to studying the kinetics of methane decomposition in arc, glow, barrier, and spark discharges. Thus, in [5], the conversion of methane in a barrier discharge in the presence of carbon dioxide was investigated. Carbon dioxide was added in order to delay the precipitation of soot and raise the conversion efficiency. The decomposition products contained a relatively small amount of acetylene; i.e., acetylene was not the main product of methane conversion in a barrier discharge. In this respect, the conversion of methane in a barrier discharge is very different from that in arc, corona, and microwave discharges. In [6], methane was decomposed in a reactor operating with both corona and spark discharges. The most energy was released during a spark discharge. The conversion of methane into acetylene was found to be very efficient, the acetylene fraction in the reaction products being about 85%. This allowed the authors of [6] to assert that their reactor can be successfully used in industry. In [7], the formation of CH_x radicals in a spark discharge in methane

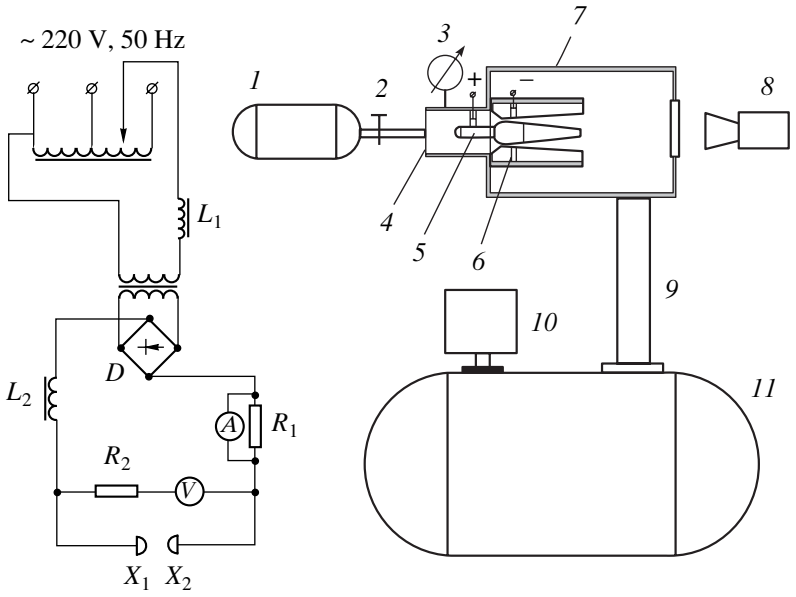

Fig. 1. Circuit diagram and schematic of the experimental setup: (*1*) high-pressure vessel, (*2*) electromagnetic valve, (*3*) manometer, (*4*) fore-chamber, (*5*) anode at the central pylon, (*6*) annular cathode, (*7*) working chamber, (*8*) photographic camera, (*9*) diffuser, (*10*) vacuum pump, (*11*) vacuum tank, (L_1, L_2) choke coils, (*D*) diode rectifier, (R_1, R_2) resistors, and (X_1, X_2) discharge electrodes.

at atmospheric pressure was simulated numerically. The discharge model described the stage of streamer propagation and the subsequent high-current stage, during which free radicals were produced. The results of simulations allowed the authors of [7] to conclude that, in a spark discharge at atmospheric pressure, a fairly high rate of CH_x production can be achieved. The oxidation of hydrocarbons in their mixtures with oxygen and air under the action of a nanosecond pulsed volume discharge was studied in [8]. Interest in the ignition of combustible mixtures under the action of nonequilibrium plasma stemmed from their application in hypersonic aircraft engines. Time-resolved and integral measurements of the spectral line intensities of molecules, molecular ions, and radicals were performed. The methane concentration was measured from the absorption of He–Ne laser radiation. It was shown that methane oxidized completely under the action of a discharge. It was also noted that methane oxidized nearly twice as slowly as other hydrocarbons.

Buyanov et al. [9] were the first to propose that hydrocarbon be decomposed in a supersonic gas-dynamic reactor, the decomposition reaction being initiated by a direct shock. To intensify the production of radicals participating in the decomposition of hydrocarbons, they suggested that a low-temperature plasma source be placed in a gas flow. It is this scheme that is used in the present paper to explore the possibility of igniting a stable uniform transverse discharge in a supersonic methane flow.

2. EXPERIMENT

To solve the problem formulated above, we created an experimental setup consisting of a power supply unit, pumping and gas supply systems, a discharge chamber, and diagnostic equipment. The setup operates as a supersonic wind channel with exhaust into a vacuum tank. The working gas (air, methane) is supplied from a high-pressure (10- to 30-atm) vessel into a forechamber through a set of valves and, then, into the working section through a supersonic nozzle (Fig. 1). The diffuser of the wind channel is attached to this section at an angle of 90° to the nozzle axis; this allows us to visually monitor the state of a discharge in the nozzle. The supersonic nozzle is formed by the central anode fixed at a pylon and by the outer annular cathode. The ignition of a volume diffuse discharge in a high-speed gas flow involves some difficulties. One of the early works devoted to experimental studies of the properties of a discharge in a supersonic air flow was [10]. The difficulties associated with igniting diffuse discharges are caused by the initial perturbations and instabilities of the flow [11–13]. For this reason, the design of the electrodes was refined so as to achieve a diffuse discharge. The use of electrodes with sharp edges can substantially stabilize the discharge. For this purpose, geometric sharpeners in the form of stepwise teeth were made at both the cathode and the anode. A scheme of the discharge arrangement in the interelectrode gap is shown in Fig. 2. In these experiments, we used a scheme with an outer cathode and a central anode, forming a supersonic flow. Our experiments have shown that a diffuse discharge depends substantially on the state of the front edges of the sharpeners

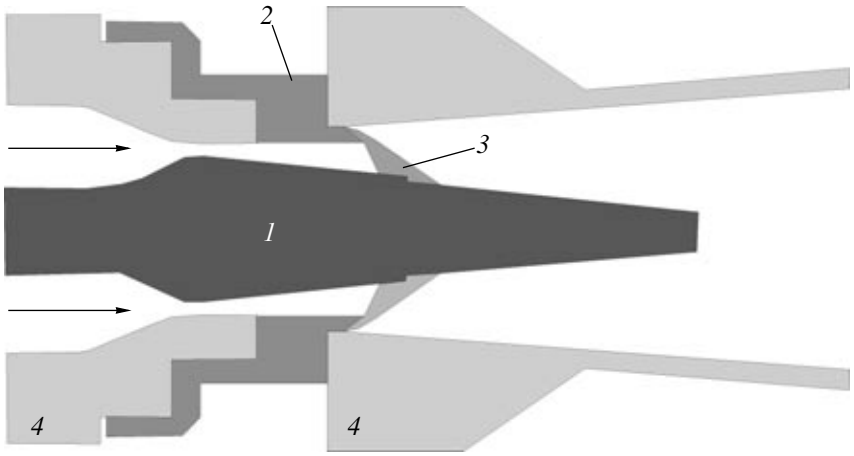

Fig. 2. Discharge in the interelectrode gap: (*1*) anode, (*2*) cathode, (*3*) discharge, and (*4*) insulator. The arrow indicates the flow direction.

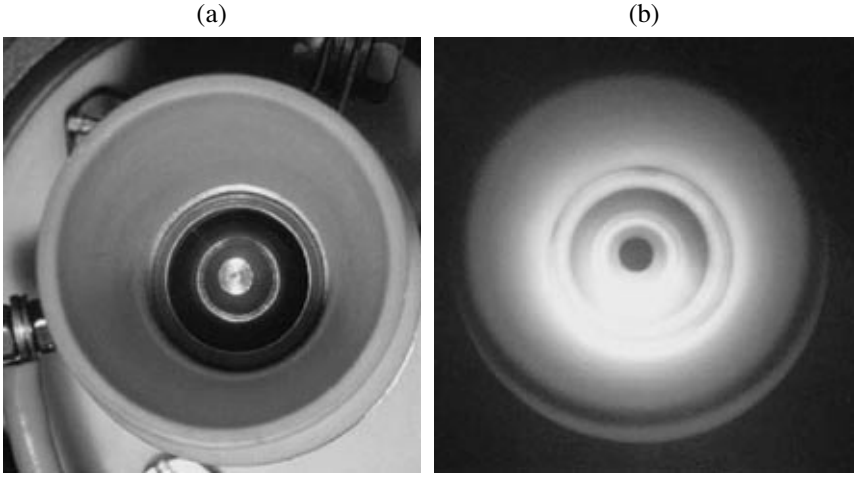

Fig. 3. (a) Photograph of the electrode unit from the side of the diffuser and (b) diffuse discharge in air.

and their positions in the flow. The design of the electrode system allowed us to efficiently cool the outer cathode and, thus, to delay the onset of thermal instability, which can lead to discharge contraction. The discharge current was maintained by a dc source (rectified ac mains voltage). The electric circuit included choke coils for discharge stabilization. The gas accelerator was tested in air in the gas-dynamic section of the wind channel, operating in a repetitive mode with exhaust into the vacuum tank. The Pitot pressure in the forechamber was 0.5 atm, the air flow rate was 10 g/s, and the Mach number of the flow at the nozzle exit was $M = 3$. A diffuse volume electric discharge that was initiated in a divergent channel filled the whole cross section of the supersonic gas flow (Fig. 3). The discharge remained diffuse during the entire operating time of the wind channel (60 s). It can be seen from Fig. 4a that the discharge current has a distinct pulsed component. The current–voltage (I–V) characteristic of the discharge is shown in Fig. 4b. It is seen that the I–V characteristic is horizontal, which is typical of glow discharges. The effect of the normal current density was observed: first, the discharge filled a certain sector of the flow, and then, as the current increased, the area filled by the discharge increased in proportion to the current until the discharge filled the whole cross section of the flow.

Similar studies were carried out with a methane flow. To determine the composition of the working gas, we performed a chromatographic analysis, the results of which are presented in the table. It can be seen that the content of hydrocarbons other than methane was lower than 1.5%.

	CH_4	C_2H_6	C_3H_8	C_2H_2	C_4H_{10}
vol %	98.7	0.76	0.35	0.1	0.09

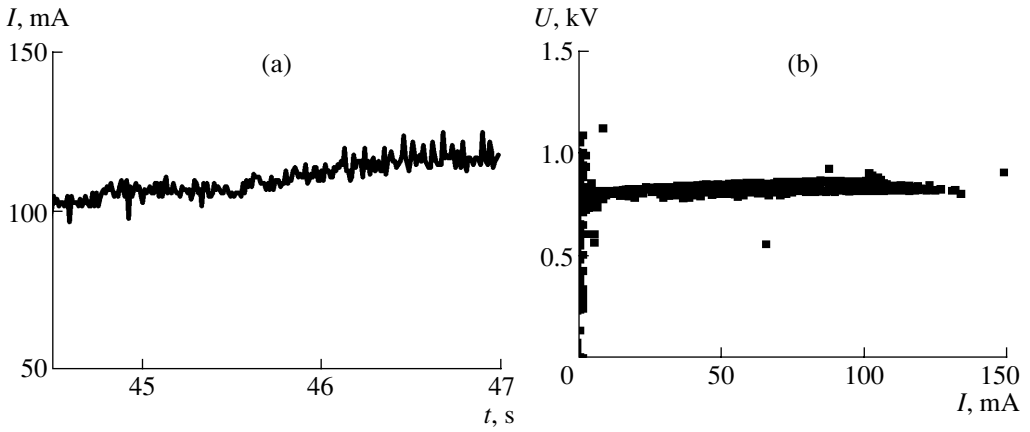

Fig. 4. (a) Waveform of the current in a discharge in air and (b) *I–V* characteristic of a discharge in air.

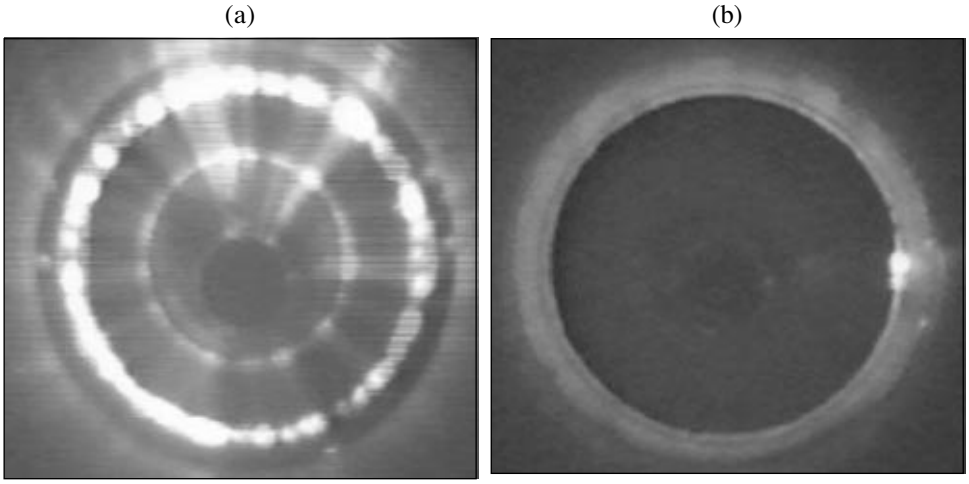

Fig. 5. Glow discharges in supersonic methane flows: (a) constricted discharge and (b) diffuse discharge.

A series of experiments on the initiation of glow discharges in methane flows demonstrated that discharges in methane (unlike those in air) show a tendency to transition into a constricted mode. The discharge in a supersonic gas flow emerging from the divergent nozzle was maintained for 5 s. The Mach number increased from 1.7 at exit from the cathode section to 3.0 at the exit from the anode section. During the first second, the discharge operated in a constricted mode (Fig. 5a). Then, a diffuse discharge with a well-defined cathode-sheath glow was established (Fig. 5b); however, it periodically returned for several tenths of a second to a constricted mode. The discharge current was 50 mA, and the voltage across the discharge gap was 0.4 kV. There was no way to achieve a stable diffuse discharge, except by decreasing the pressure in the fore-chamber to 0.2 atm.

3. THEORY AND ESTIMATES

A comprehensive self-consistent model of a discharge in a supersonic molecular-gas flow should include calculations of the cathode and anode regions (with allowance for the complicated configuration of the electrodes) and the ion–molecular and chemical kinetics of the processes occurring in a discharge. The reason that such a model is still lacking is not only its complexity, but also the lack of data on the cross sections for elementary processes in many gases.

In this paper, we consider a steady-state transverse discharge initiated in a supersonic methane flow. In a one-dimensional approximation for the flow of a compressible gas through the nozzle, we estimated the characteristics of the flow in the region where the discharge was initiated. The gas temperature in the discharge was 190 K, and the gas pressure was on the order of 10 and

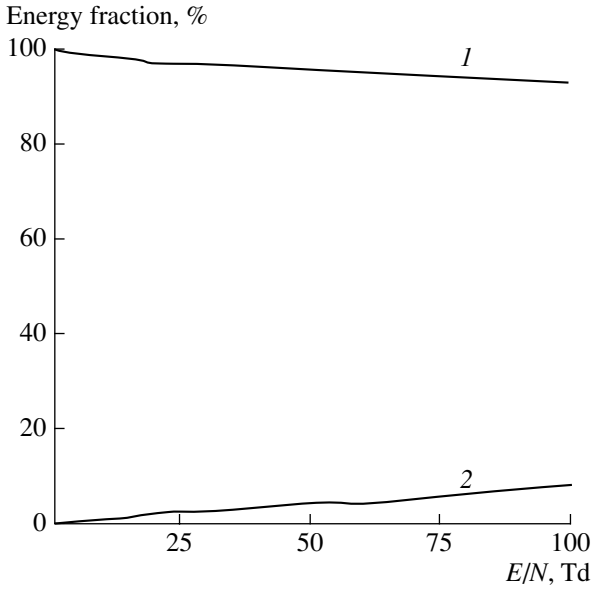

Fig. 6. Distribution of the energy deposited in a glow discharge in methane: (*1*) energy fraction spent on the vibrational excitation of methane molecules and (*2*) energy fraction spent on dissociation, ionization, and elastic collisions as functions of *E*/*N*.

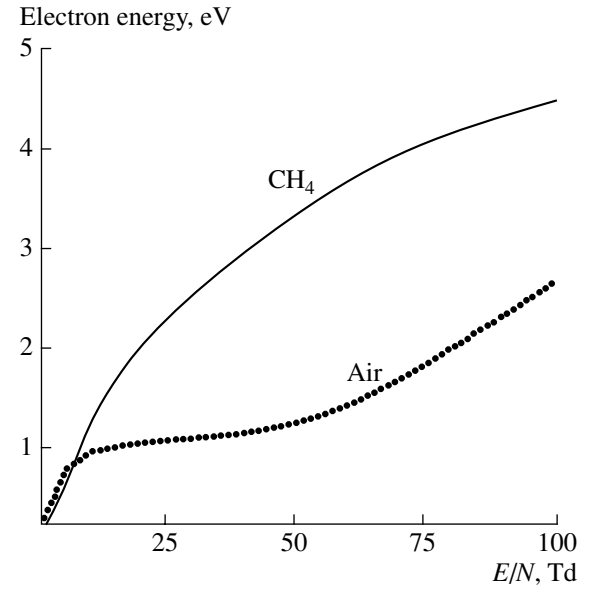

Fig. 7. Characteristic electron energy calculated from the Boltzmann equation as a function of *E*/*N*.

4 Torr, which corresponded to forechamber pressures of 0.5 and 0.2 atm, respectively.

For a comparative analysis of the formation of a glow discharge in air and methane, we calculated the energy characteristics and the electron transport parameters by solving the Boltzmann equation for the electron energy distribution function in a two-term approximation [14]. For this purpose, we compiled a database in which we included the cross sections for elastic and inelastic electron collisions with methane molecules. The excitation of two vibrational modes of CH_4 molecules with energies of 0.162 and 0.361 eV were taken into consideration. The electronically excited methane molecules are unstable and undergo dissociation. Thus, our calculations included the cross sections for vibrational excitation; the transport cross section for elastic scattering (which has a characteristic Ramsauer minimum); the ionization cross sections for the production of CH_4^+ ions (with a threshold energy of 12.61 eV) and CH_3^+ ions (with a threshold energy of 14.3 eV), and the dissociation cross sections for the production of CH_3, CH_2, CH, and C radicals. The threshold energies for methane dissociation lie in the range 9–12 eV. The values of the above cross sections were taken from [15–17]. Figure 6 shows the energy fraction spent on the vibrational excitation of methane molecules and that spent on dissociation, ionization, and elastic collisions as functions of the parameter *E*/*N* in a discharge. It can be seen from Fig. 6 that, in the given range of *E*/*N* values, the deposited energy goes into the vibrational excitation of methane molecules. It is well known that discharges in air in the same range of parameters exhibit similar features. The *V*–*T* relaxation time of nitrogen and methane molecules is substantially longer than the time during which the gas passes through the discharge. Therefore, the vibrational energy has no time to convert into translational energy, so the gas temperature in the discharge is low. Since the plasma is nonequilibrium, the electron temperature differs substantially from the gas temperature. Figure 7 presents results of calculations of the so-called characteristic electron energy for discharges in air and methane. The characteristic electron energy was calculated from the Einstein ratio for the electron diffusion and mobility, $\varepsilon = D_e/(e\mu_e)$. It can be seen that the electron energy increases with increasing parameter *E*/*N*. Note that, starting from $E/N \sim 15$ Td, the characteristic electron energy for a discharge in methane is substantially larger than that for a discharge in air. This may be attributed to the methane molecule having no stable electronically excited states. The threshold energies for dissociation and ionization are fairly large (9–12 eV), which, in turn, results in large values of the average and characteristic energies. We studied the properties of electron transport in a discharge. Figure 8 compares the electron drift velocities v_{dr}^{air} and $v_{dr}^{CH_4}$ as functions of the reduced field for discharges in air and in methane. The difference is that the drift velocity in air is a monotonically increasing function of *E*/*N*, whereas the drift velocity in methane is a nonmonotonic function. Such behavior of the drift velocity in methane is related to the fact that the energy corresponding to the Ramsauer minimum in the cross section for elastic collisions in methane is close to the vibrational energy of a methane molecule. A similar sit-

uation takes place in discharges in noble gases with additives of molecular gases. It is well known that, when the derivative $\partial v_{dr}/\partial(E/N)$ is negative, the discharge is unstable against the development of striations [18]. The coincidence of the energy corresponding to the Ramsauer minimum with the vibrational energy of the methane molecule makes it necessary to more thoroughly examine the results of solving the Boltzmann equation in the two-term approximation. A comparative analysis of the results of calculations in the two-term approximation, Monte Carlo calculations, and experimental data was performed in [15]. It was shown that, for a discharge in methane, the two-term approximation can lead to a substantial error when the average electron energy is close to the energy corresponding to the Ramsauer minimum. Such a situation occurs at $E/N \sim 3$ Td. Under our experimental conditions, the reduced field E/N is considerably larger and calculations in the two-term approximation yield adequate results. Figure 8 also shows the measured values of the electron drift velocity [15]. It can be seen that the calculated results agree well with the experimental data. Figure 9 shows the calculated coefficient of ionization of methane molecules as a function of E/N. The coefficient of dissociation is larger than that of ionization by one to two orders of magnitude. It is well known that the electron-impact dissociation of methane leads to the production of chemically active radicals. The characteristic times of chemical interactions are 10^{-2}–10^{-3} s. The transit time of methane molecules (and radicals) through the discharge region is on the order of 10^{-5} s. Therefore, chemical conversions in the discharge can be ignored.

Let us analyze the conditions under which a diffuse discharge operates in methane. The parameters of the positive column of a quasi-steady discharge in a cross section that lies nearly at the mid-distance from the cathode and anode are described by the balance equations for the electron density,

$$-\nabla \cdot (D_a \nabla n_e) = k_e n_e N - \beta n_e^2; \quad (1)$$

the electron energy,

$$\sigma E^2 = N k_{vib} \varepsilon_{vib}; \quad (2)$$

and the electron current,

$$\int e v_{dr} n_e dS = i. \quad (3)$$

Here, n_e is the electron density, N is the number density of the gas molecules, D_a is the coefficient of ambipolar diffusion, k_e is the coefficient of gas ionization via inelastic collisions of electrons with gas molecules, β is the coefficient of volume recombination, σ is the plasma conductivity per electron, k_{vib} is the rate of vibrational excitation, ε_{vib} is the vibrational quantum energy, E is the electric field strength, v_{dr} is the electron drift velocity, i is the current in the external circuit, and dS is the area element of the cross section of the plasma column.

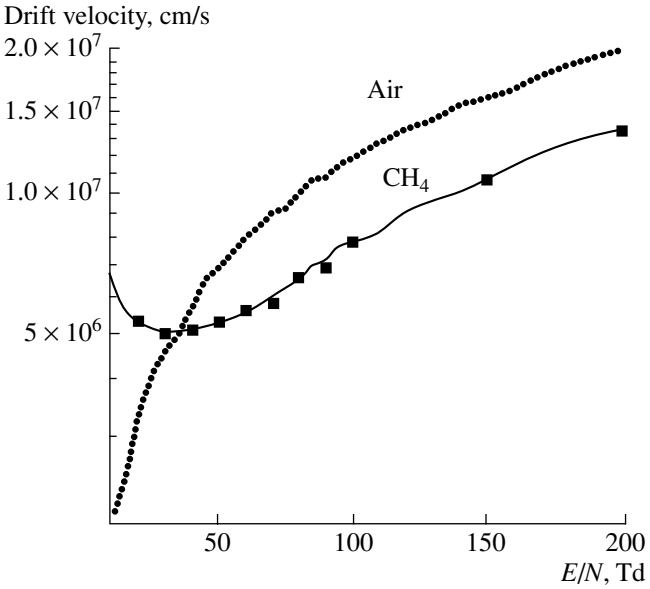

Fig. 8. Electron drift velocity in air and methane vs. E/N. The curves show the drift velocity calculated from the Boltzmann equation, and the symbols show the experimental data [18].

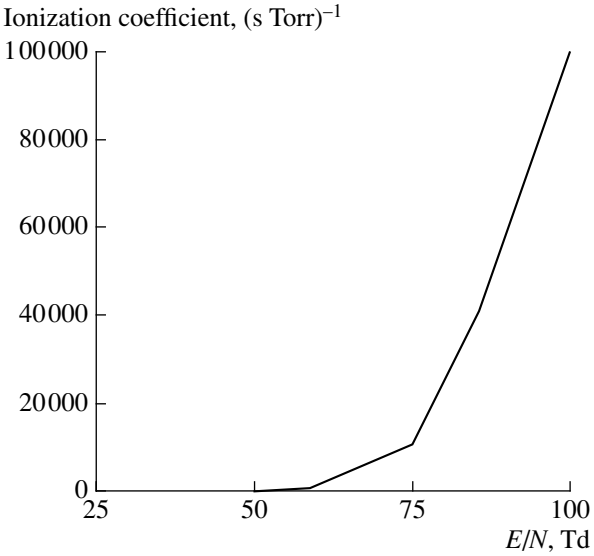

Fig. 9. Coefficient of ionization of methane molecules vs. E/N.

By solving the set of Eqs. (1)–(3), we can estimate the value of E/N in the positive column of a glow discharge in methane, the characteristic diffusion length Λ, and the electron density. Estimates were made for a gas pressure of 4 Torr. From Eq. (2), taking into account the dependences of the conductivity σ and the coefficient k_{vib} on E/N, we find that the reduced field in the positive column is about 60 Td.

The transverse size of the region filled by the discharge between the cathode and anode is determined by

the diffusion length Λ, which was estimated from Eq. (1) under the assumption that diffusion dominated over volume recombination. The coefficient of ambipolar diffusion was estimated from the expressions

$$D_a = D_i \frac{T_e}{T_g}, \quad (4)$$

$$D_i = \mu_i \frac{kT_g}{e}, \quad (5)$$

where D_i is the coefficient of ion diffusion; T_e and T_g are the electron and gas temperatures, respectively; μ_i is the mobility of methane ions in the parent gas; e is the electron charge; and k is the Boltzmann constant. The value of the mobility μ_i was taken from [16], where it was determined experimentally. For comparison, the coefficient of ion diffusion was also estimated by using the classical expression

$$D_i = \frac{\lambda_i v_i}{3}. \quad (6)$$

Here, λ_i is the ion mean free path length, which is determined by one of the fastest processes—the conversion of the original CH_4^+ and CH_3^+ ions into the more complex CH_5^+ and $C_2H_5^+$ ions, the conversion rate being proportional to the density of methane molecules. Therefore, the ambipolar diffusion coefficient is inversely proportional to the gas density in the flow. The values of the diffusion coefficient calculated by expressions (5) and (6) are in good agreement. The resulting estimate of the characteristic transverse size of the plasma column is about 0.3 cm. This estimate agrees with the visually observed transverse size of the discharge glow. The estimated electron density in the discharge is on the order of 10^{10}–10^{11} cm^{-3}.

As was noted above, diffuse discharges in our experiments were unstable and periodically returned to a constricted mode. It is was difficult to visually detect the region where the instability originated. The problem of discharge instability, namely, its transition into a constricted mode, was thoroughly analyzed in [19, 20]. There are many different mechanisms for the onset of discharge instabilities. Among them, thermal instabilities associated with gas heating in a discharge are presently best understood. On the other hand, mechanisms for the onset of instabilities associated with electrode-sheath phenomena have been investigated very poorly. We believe that, in our experiments, the onset of thermal instability is hardly probable. Let us consider possible mechanisms for the onset of volume instabilities. There are two phenomenological attributes of volume instability: (i) charge particles are mainly produced near the axis of a discharge, and (ii) their loss by diffusion is small compared to that by volume recombination. For the onset of instability in a discharge in a gas flow, it is also necessary that the time during which the instability develops be shorter than the time during which the particles escape from the discharge. The latter is on the order of $\tau_u = \Lambda/u$, where Λ is the characteristic transverse size of the discharge and u is the flow velocity. Under our experimental conditions, we have $\tau_u \sim 10^{-5}$ s. Hence, a transition of the discharge into a constricted mode may be caused by processes with characteristic times of $\tau \ll 10^{-5}$ s. Taking into account the ranging of elementary processes in their characteristic times [19], we can infer that such processes may be, e.g., dissipation of the average electron energy and electron–electron collisions, resulting in the relaxation of the electron distribution function to a Maxwellian one.

Let us consider the conditions under which volume recombination dominates over ambipolar diffusion. This condition can be written in the form

$$\beta n_e \gg \frac{D_a}{\Lambda^2}. \quad (7)$$

In electropositive molecular gases, charged particles are usually neutralized via dissociative recombination. According to the data from [21], the coefficient β is on the order of $\sim 10^{-6}$ s^{-1}. The values of the electron density, the coefficient of ambipolar diffusion, and the drift length Λ were estimated above. Substituting these values into condition (7), we find that its left-hand side is comparable in order of magnitude to the right-hand side. This means that, in our experiments, conditions for a transition of the discharge from a diffuse to a constricted mode could indeed be satisfied. A decrease in the gas pressure leads to an increase in the coefficient of ambipolar diffusion, thereby facilitating the operation of a diffuse discharge. Nevertheless, we cannot unambiguously answer the question of the type of instability (volume or electrode) that takes place under our experimental conditions. This problem requires further investigation.

4. CONCLUSIONS

Transverse glow discharges in supersonic air and methane flows have been studied experimentally and theoretically. The results of these studies show that a stably operating diffuse discharge in air fills the whole cross section of the flow. In contrast, a discharge in methane shows a tendency to transition into a constricted mode. The parameters of the plasma and the electric field have been estimated. The estimates show that, under our experimental conditions, the discharge operates in a regime that is transient between a diffuse and a constricted discharges. The problem of determining the mechanism for the onset of instability requires further investigation.

ACKNOWLEDGMENTS

This work was supported in part by the Presidium of the Russian Academy of Sciences (program no. 20) and

the Siberian Division of the Russian Academy of Sciences (integration project no. 122).

REFERENCES

1. V. M. Fomin, A. V. Lebedev, and A. I. Ivanchenko, Dokl. Akad. Nauk **361**, 58 (1998) [Phys. Dokl. **43**, 440 (1998)].
2. V. M. Fomin, T. A. de Roquefort, A. V. Lebedev, and A. I. Ivanchenko, Dokl. Akad. Nauk **370**, 623 (2000) [Phys. Dokl. **45**, 503 (2000)].
3. V. M. Fomin, T. A. de Roquefort, A. V. Lebedev, and A. I. Ivanchenko, Dokl. Akad. Nauk **374**, 340 (2000) [Phys. Dokl. **45**, 84 (2000)].
4. E. N. Borisova and E. N. Eremin, Zh. Fiz. Khim. **41**, 137 (1967).
5. Chang-Jun Liu, B. Hue, B. Eliasson, et al., Plasma Chem. Plasma Process. **12**, 301 (2001).
6. S. L. Yao, E. Suzuki, N. Meng, and A. Nakayama, Plasma Chem. Plasma Process. **22**, 225 (2002).
7. A. V. Kirikov, V. V. Ryzhov, and A. I. Suslov, Pis'ma Zh. Tekh. Fiz. **25** (19), 82 (1999) [Tech. Phys. Lett. **25**, 794 (1999)].
8. N. B. Anikin, S. M. Starikovskaya, and A. Yu. Starikovskiĭ, Fiz. Plazmy **30**, 1105 (2004) [Plasma Phys. Rep. **30**, 1028 (2004)].
9. R. A. Buyanov, N. A. Vasil'eva, V. N. Parmon, et al., Preprint No. 5-2001 (Inst. of Theoretical and Applied Mechanics, Siberian Division, Russian Academy of Sciences, Novosibirsk, 2001).
10. V. I. Alferov and A. S. Bushmin, Zh. Éksp. Teor. Fiz. **44**, 1775 (1963) [Sov. Phys. JETP **17**, 1190 (1963)].
11. I. G. Galeev, V. E. Goncharov, B. A. Timerkaev, et al., Teplofiz. Vys. Temp. **28**, 843 (1990).
12. G. Yu. Dautov and B. A. Timerkaev, *Generators of Nonequilibrium Gas-Discharge Plasma* (Izd. KGTU, Kazan, 1996) [in Russian].
13. A. P. Ershov, O. S. Surkont, I. B. Timofeev, et al., Teplofiz. Vys. Temp. **42**, 516 (2004).
14. L. C. Pitchford, S. V. O'Neil, and J. R. Rumble, Phys. Rev. A **23**, 294 (1981).
15. D. K. Davies, L. E. Kline, and W. E. Bies, J. Appl. Phys. **65**, 331 (1989).
16. Y. Ohmori, K. Kitamori, M. Shimozuma, and H. Tagashira, J. Phys. D **19**, 437 (1986).
17. W. L. Morgan, Plasma Chem. Plasma Process. **12**, 477 (1992).
18. *Encyclopedia of Low-Temperature Plasma*, Ed. by V. E. Fortov (Nauka, Moscow, 2000), Introductory Vol. 2, p. 58 [in Russian].
19. A. P. Napartovich and A. N. Starostin, Khim. Plazmy **6**, 153 (1979).
20. A. V. Eletskiĭ and R. V. Chiflikyan, Khim. Plazmy **15**, 266 (1989).
21. A. V. Eletskiĭ and B. M. Smirnov, Usp. Fiz. Nauk **136**, 25 (1982) [Sov. Phys. Usp. **25**, 13 (1982)].

Translated by N.F. Larionova